Compatibility of S-N and crack growth curves in the fatigue reliability assessment of a welded steel joint

Hashemi, S.B.; Maljaars, J.; Leonetti, D.; Snijder, H.H.

Document Version
Publisher's PDF, also known as Version of Record (includes final page, issue and volume numbers)

Please check the document version of this publication:

• A submitted manuscript is the author's version of the article upon submission and before peer-review. There can be important differences between the submitted version and the official published version of record. People interested in the research are advised to contact the author for the final version of the publication, or visit the DOI to the publisher's website.
• The final author version and the galley proof are versions of the publication after peer review.
• The final published version features the final layout of the paper including the volume, issue and page numbers.

Link to publication

Download date: 19. Jan. 2018

2nd International Conference on Structural Integrity, ICSI 2017, 4-7 September 2017, Funchal, Madeira, Portugal

Compatibility of S-N and crack growth curves in the fatigue reliability assessment of a welded steel joint

Bahman Hashemi[a],*, Johan Maljaars[a,b], Davide Leonetti[a], H.H (Bert) Snijder[a]

[a]Eindhoven University of Technology, Department of the Built Environment, P.O Box 513, 5600MB, Eindhoven, The Netherlands
[b]TNO, Delft, The Netherlands

Abstract

Reliability analysis is a crucial phase in assessing the safety status of new and existing structures. One of its applications is to predict the fatigue life of fatigue prone details. Two models are used to formulate the fatigue limit state: S-N curves in combination with Palmgren-Miner damage accumulation rule and linear elastic fracture mechanics using fatigue crack growth rate curves. Within each model, choices must be made on the values of the variables and these choices are sometimes different in different standards. This study investigates the consistency between the standards by determining the failure probability of the different models and values for a transverse butt weld joint under Variable Amplitude Loading. Partial factors required for the design are then derived as a function of the required reliability for each model and associated values. The influence of the uncertainties related to each involved variable is evaluated by performing a sensitivity analysis.

1. Introduction

Fatigue is a dominant failure mode for structures such as bridges subjected to time varying loading. Several empirical or semi-analytical fatigue resistance models have been developed since the19[th] century. Among them, the most common ones used to assess welded details are the nominal stress-life (S-N) and fatigue fracture mechanics

---

* Corresponding author. Tel.: +390402472948;
  E-mail address: s.b.hashemi@tue.nl

crack growth (LEFM) models. Most standards such as EN 1993-1-9 (2005) and BS 7608 (2014) recognize damage-tolerant design and safe-life design concepts. Damage tolerant design is based on the assumption that periodic inspection is applied aiming at detecting a fatigue crack before it grows large enough to cause failure. Inspection intervals can be determined using LEFM whereas the S-N curve is not suited for this purpose. On the other hand, safe-life design is based on the idea that the structure should withstand the applied loads for the whole design life. Because the fatigue life of welded joints is dominated by crack propagation as shown by Hobbacher (1996), both the S-N and crack growth methods can be used for the safe life concept. Since the models have a different basis but are both applied in standards, it is of interest to study the reliability for both models and to determine whether these are consistent. In this paper, this consistency is studied for a transverse butt welded-joint. The fatigue assessment models require data which are subjected to considerable uncertainties, which might be due to the stochastic nature of variables, measurement inaccuracies, modelling inaccuracy or human errors. The effect of these uncertainties can be taken into account in a probabilistic assessment using the distributions of the random variables. The appropriate distributions can be obtained from literature or by expert opinion. Several standards such as JCSS (2011) and ISO 2394 (2015) have been published to generally address the different aspects of reliability analysis problems while some others such as BS 7910 (2015) and DNV-GL (2015) present reliability analysis techniques specifically for fatigue evaluations. These standards provide general distributions of the variables in the S-N and fracture mechanics models that have been used in this paper. To avoid the complexity caused by dealing with random variables in practical designs, standards for fatigue design such as EN 1993-1-9 allow to assess the structure with a deterministic model in combination with partial factors. To reach the desired reliability, the uncertainty level of the assessment as well as the consequences caused by failure are contemplated in the partial factors. Partial factors for each model and for several required reliability levels are derived in this paper using equal distributions and the consistency between S-N and FM models in different standards is discussed.

2. Probabilistic fatigue assessment

2.1. S-N curve approach

S-N curves are derived by fitting a proper model to the data obtained from constant amplitude (CA) fatigue tests. These models relate the CA applied stress range ($\Delta\sigma$) greater than the constant amplitude fatigue limit (CAFL) to the corresponding required number of cycles to failure (N) in an S-N curve of the following form:

$$\log(N) = \begin{cases} \log(a_1) - m_1 \log(\Delta\sigma) & \text{for } \Delta\sigma > CAFL \\ \infty & \text{for } \Delta\sigma \leq CAFL \end{cases} \tag{1}$$

Where a_1 and m_1 are parameters related to the material and the detail's geometry. For variable amplitude (VA) loading, the S-N curve is modified into:

$$\log(N) = \begin{cases} \log(a_1) - m_1 \log(\Delta\sigma) & \text{for } \Delta\sigma > \Delta\sigma_D \\ \log(a_2) - m_2 \log(\Delta\sigma) & \text{for } \Delta\sigma \leq \Delta\sigma_D \end{cases} \tag{2}$$

The S-N curves proposed for a transversely loaded butt weld are those corresponding to so-called detail categories 80 and E, respectively, in EN 1993-1-9 and BS 7608. Their main differences are the different position of the constant amplitude fatigue limit (CAFL), the different value of the probability of exceedance associated to the characteristic S-N curve and the extension of the curve below the CAFL to consider variable amplitude (VA) loading. In both standards, the negative inverse slopes have values of $m_1 = 3$ and $m_2 = m_1 + 2$ according to Haibach's proposal (1970). The values of a_1 are almost equal. In EN 1993-1-9, the CAFL is defined at $N = 5 \times 10^6$ cycles for CA loading and for VA loading, the knee-point is defined at a stress range $\Delta\sigma_D$ taken equal to the CAFL. A cut-off value is further defined at $N = 10^8$ cycles. On the other hand, the CAFL in BS 7608 is defined at $N = 10^7$ cycles and the VA S-N

curve has a knee-point $\Delta\sigma_D$ defined at $N = 5 \times 10^7$ cycles, thereby following the modified Haibach rule proposed by Niemi (1997). Fig.1 shows the S-N curves for the detail 80 in EN 1993-1-9 and the category E in BS 7608, both given for a probability of exceedance equal to 0.05.

In many civil engineering structures including bridges, loading is in the form of VA, caused by time varying loads of different magnitude. The stress history is transformed into a spectrum that relates each stress range $\Delta\sigma_i$ to the corresponding counted number of cycles n_i by means of a counting method, e.g. rainflow or reservoir methods and the fatigue damage is quantified in term of Miner's damage summation. According to this rule, all stress cycles cause proportional fatigue damage which is linearly additive:

$$D_n = \sum_i d_i = \sum_i n_i \Big/ N_i \tag{3}$$

where D_n is the damage due to $n = \sum_i n_i$ cycles, d_i is the damage caused by all stress cycles with range $\Delta\sigma_i$ and N_i is the number of cycles to failure for that same stress range obtained from the S-N relation (2). If the maximum stress range is smaller than the CAFL, it is assumed that fatigue failure does not occur. In tests, this situation is referred to as run-out.

2.2. Linear elastic fracture mechanics approach

In a LEFM based fatigue assessment, the stress intensity factor (SIF) is the governing damage driving parameter. It describes the intensity of the stress state at the crack tip in elastic condition and can also be applied with good approximation in case of small-scale plasticity. The generic SIF formulation for a weld toe surface crack, with depth a and width $2c$, under primary uniaxial state of stress perpendicular to the crack face can be expressed by BS 7910:

$$\Delta K_I = Y_f \left\{ M_{km} M_{mm} \Delta\sigma_m + M_{kb} M_{mb} \left[\Delta\sigma_b + (\mathrm{k}_m - 1)\Delta\sigma_m \right] \right\} \sqrt{\pi a} \tag{4}$$

where Y_f is the plate width correction factor; M_k is the SIF magnification factor that takes into account the weld geometry; M_m is the correction factor for an elliptical crack that takes into account the effect of the stress redistribution in the ligament; k_m is the misalignment factor and σ is the remote applied stress. The subscripts m or b refer respectively to membrane or bending loading. The fatigue crack growth rate (FCGR) is related to the SIF range ($\Delta K = K_{max} - K_{min}$) resulting in the FCGR relation, which has been divided into three stages. (a) The near-threshold or slow crack-growth region, for ΔK approaching its threshold value (ΔK_{th}) for which no propagation is assumed to happen (run-out). (b) The stable crack-growth region in which the logarithm of the FCGR increases almost linearly with the logarithm of the Stress Intensity Factor range. (c) The unstable crack-growth region, for ΔK approaching its critical value (ΔK_c) which is related to the critical Stress Intensity Factor (K_C or K_{IC}), depending on the stress state. Stage (c) is not considered in this paper for reasons of simplicity. The FCGR in stage II is represented using the power law relation known as simplified relation:

$$\frac{da}{dN} = A\Delta K^q \quad for \ \Delta K > \Delta K_{th} \tag{5}$$

In which da/dN is the crack depth increment per cycle. Variables q and A are material constants obtained by tests. The former only depends on the material; the latter depends on the loading conditions as well. In order to take into account the near-threshold crack growth rate stage, a bilinear relation is suggested in BS 7910 instead of the Simplified relation:

$$\frac{da}{dN} = \begin{cases} 0 & for \ \Delta K \leq \Delta K_{th} \\ A_1 \Delta K^{q_1} & for \ \Delta K_{th} < \Delta K \leq \Delta K_{tr} \\ A_2 \Delta K^{q_2} & for \ \Delta K > \Delta K_{tr} \end{cases} \tag{6}$$

where ΔK_{th} is the Stress Intensity Factor range below which no crack propagation is assumed to occur and ΔK_{tr} is the value that separates the first and the second stage of the FCGR relation (Fig. 1).
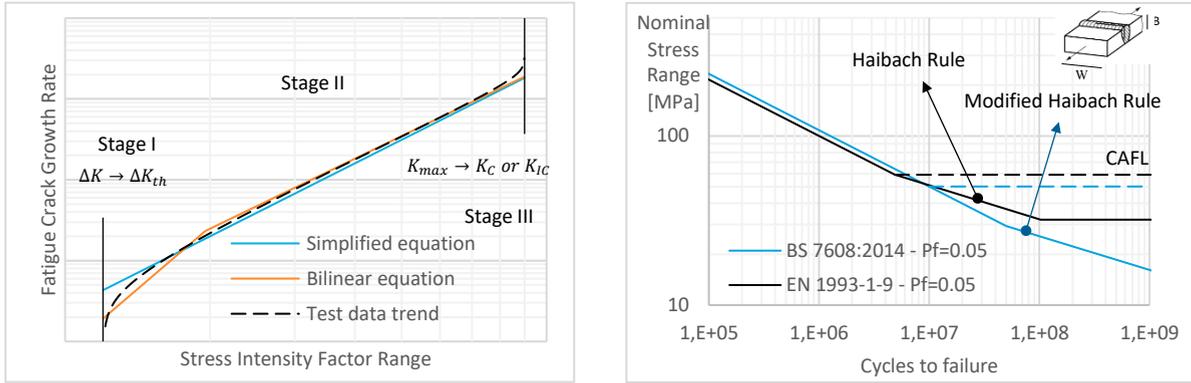
Fig. 1 Fatigue crack growth rate curve (Left), S-N curves proposed in BS 7608:2014 for class E and in EN 1993-1-9 for detail 80 (Right)

In a similar approach, the SIF and crack increment at the plate surface (with direction of the crack) can be calculated. By substituting (4) into (5) or (6) and solving the differential equations through an incremental numerical procedure, a relationship between the number of cycles, *N,* and the crack dimensions, *a* and *c,* results.

2.3. Variable amplitude loading stress spectrum

A stress histogram, following a Rayleigh probability density function, as proposed by Gurney (2006), has been selected for the analysis. The stress spectrum is characterized by the root mean square stress range, $\Delta S_{rms} = 35.6\ MPa$ and includes $n = 23$ stress ranges within the interval $[\Delta S_{min} = 3.55\ MPa; \Delta S_{max} = 160\ MPa]$.

3. Reliability analysis

In general, the first step in a reliability analysis is to define the limit state function $g(X) = R - L$ where X is the vector containing all random parameters and R and L represent the resistance and load effects, respectively. Failure occurs when $g(X) < 0$. The failure probability P_f, and the corresponding reliability index β, are defined as:

$$P_f = P\big[g(\mathrm{X}) < 0\big] = \int\limits_{g(\mathrm{X})<0} f_x(\mathrm{X})\,\mathrm{d}x \tag{7}$$

$$\beta = -\Phi^{-1}(\mathrm{P}_f) \tag{8}$$

where $\boldsymbol{f_x(X)}$ is the multivariable probability density function of X and $\boldsymbol{\Phi^{-1}}(.)$ is the inverse cumulative normal distribution function. In this study, Crude Monte Carlo Simulation (CMCS) is used to approximate the integral in (7).

3.1. Limit state in S-N approach

The time dependent limit state function can be defined as:

$$g(\mathrm{X}, \mathrm{t}) = \mathrm{D}_{cr} - D_n \tag{9}$$

where X is the vector of random variables, *t* the time, D_{cr} is the critical Miner's damage sum at failure and D_n is the damage due to *n* cycles. Random variables in this approach as well as constant parameters are presented Table 1. This table also provides the characteristic values (X_k) used in the deterministic calculations (Section 4.1). The reliability

analyses were performed using CMCS with 3×10^6 samples. For each sample, VA loads are applied until reaching the limit state condition. The total number of applied cycles (N) at failure is stored. By using the Kaplan-Meier (1958) estimator the trend of failure probability over lifetime is derived.

3.2. Limit state in LEFM approach

In general, there are two possible ways to define the limit state criteria in LEFM approach; 1) Fracture criterion. 2) Critical crack size criterion. In this study, for simplicity, fatigue life is predicted by the second criterion which can be formulated as: $g(X, t) = \min[a_{cr} - a_n, c_{cr} - c_n]$, where the critical crack has assumed dimensions $a_{cr} = 0.9B$ and $c_{cr} = 0.45W$, variables B and W being the plate thickness and width equal to 25 mm and 100 mm, respectively. The crack depth and semi width at n cycles are denoted as a_n and c_n, respectively. Distribution functions for the random variables as well as the characteristic parameters to be used in a deterministic calculation are shown in Table 2.

Table 1. Distribution functions for random variables in S-N approach (unit: MPa).

Variable		Distribution	μ	COV	Ref	X_k
$Log(a_1)$[a]	Material parameter 1st line – EN1993 model	Normal	12.42	0.02	[b]	$\mu(1-2COV)$
	BS7608 model		12.52	0.02	BS 7608	
$Log(a_2)$[a]	Material parameter 2nd line – EN1993 model	Normal	16.24	0.02	[b]	$\mu(1-2COV)$
	BS7608 model		15.73	0.02	BS 7608	
m_1	Slope value 1st line	Deterministic	3.0	-	EN 1993 & BS 7608	μ
m_2	Slope value 1st line	Deterministic	5.0	-	EN 1993 & BS 7608	μ
D_{cr}	Miner's sum at failure	Lognormal	1.0	0.3	JCSS	μ

[a] a_1 and a_2 are fully correlated.   [b] The same scatter as detail category E in BS7608 is assumed.

Table 2. Distribution functions for random variables in LEFM (units: N, mm).

Variable		Distribution	μ	COV	Ref	X_k
A_1 (air)[a, b]	Stage I parameter – Bilinear model	Lognormal	4.8×10^{-18}	1.70	HSE (1998)	$\mu(1+2COV)$
A_2 (air)[a, b]	Stage II parameter- Bilinear model	Lognormal	5.86×10^{-13}	0.60	HSE	$\mu(1+2COV)$
A (air)[a]	model Parameter in Simplified model	Lognormal	2.5×10^{-13}	0.54	HSE	$\mu(1+2COV)$
q_1	Slope value of stage I	Deterministic	5.10	-	HSE	μ
q_2	Slope value of stage II	Deterministic	2.88	-	HSE	μ
q	Slope value of simplified relation	Deterministic	3.00	-	HSE	μ
ΔK_{th} (air)	Threshold value for ΔK	Lognormal	140	0.4	JCSS	$\mu(1-2COV)$
a_0	Initial crack depth	Lognormal	0.15	0.66	JCSS	μ
a_0/c_0	Initial crack ratio	Lognormal	0.62	0.4	JCSS	μ

[a] stress ratio $\sigma_{min}/\sigma_{max} \geq 0.5$.   [b] A_1 and A_2 are fully correlated.

The reliability analyses were performed using CMCS with 3×10^6 samples. For each sample, starting from a random initial crack size representing as-welded conditions with dimensions a_0 and c_0, the semi-elliptical crack grows under VA loading until either the crack depth or the crack width reaches its critical value. The failure probability over lifetime is derived in a similar way as used for the S-N model.

4. Results and discussion

The failure probability and the reliability index over lifetime are shown in Fig.2 for both models. The discrepancy in the reliability trends among S-N models is attributed to the difference in 1) the CAFL position; 2) the method

employed to consider VA loading, as shown in Fig. 1. In the region with number of cycles $< 5x10^5$, the accuracy of the results is a bit too low due to an insufficiently large number of CMCS samples. However, that region is not of interest in this study as the reliability is extremely large and not realistic for practical designs. In case of the S-N approach based on EN 1993, 583 MC samples (0.0002%) behaved as run-out whereas for the BS 7608 based model, this number is 16. Therefore, for the selected stress spectrum and detail, the threshold condition in S-N models is not noticeably effective. On the other hand, the threshold condition for the LEFM models plays an important role since 11.93% of the samples fall into the run-out category. This can be observed in the graphs of Fig. 2 where the failure probability for LEFM tends to 0.9 instead of 1 and the reliability index has a horizontal asymptote in the region with high number of cycles (~>50 millions). It can be observed that for a number of cycles located in a certain range (~1–6 millions) the curves are following almost the same trend. This area is of interest because of the reliability index being in the range of the target values set by standards for bridges.
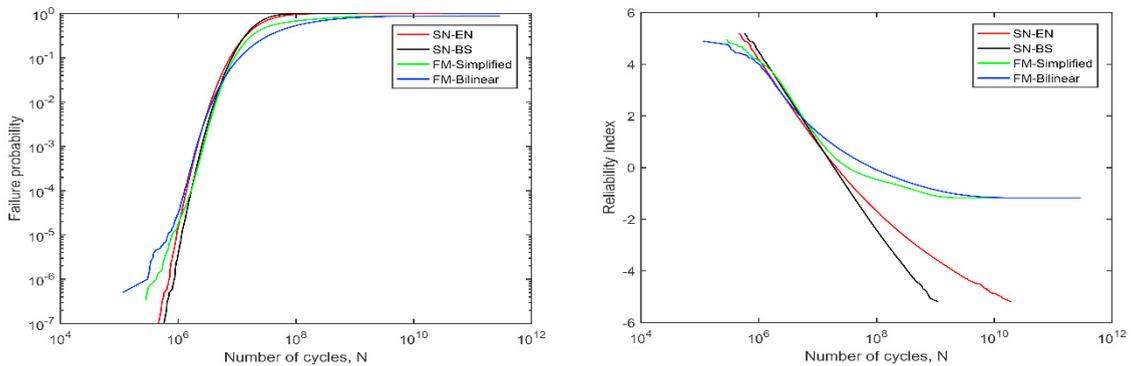
Fig. 2 Failure probability trend over life time (Left), Reliability index trend over life time (Right)

4.1. Partial Factors

The partial factors are calibrated by the same approach described by Maljaars et al. (2012), i.e. a deterministic calculation is applied using the characteristic values of the variables whereby the fatigue strength is divided by a partial factor that is selected in such a way that the number of cycles agrees with that according to Fig. 2 for a given reliability index. Because scatter is considered on the variables of the resistance side only, and not on the load side, the target reliability indices recommended by EN 1990 (2002) are multiplied by a weight factor α_R factor which is taken as 0.8 in agreement with EN 1990. The partial factor values for different values of the target reliability index and for each fatigue assessment method as well as the fatigue life (N_k) obtained by using the characteristic value of parameters (X_k) for each model are reported in Table 3.0. The fatigue life for all models are located in the zone where the curves in Fig. 2 are comparable. Consequently, the partial factors for each reliability level are comparable for the different models (less than 10% difference).

4.2. Sensitivity Analysis

In order to study the influence of each variable on the fatigue reliability of the detail, a sensitivity analysis has been performed by defining several simulations (Table 4). In each simulation, the desired parameter is considered as a deterministic value (X_k in Tables 1 & 2) instead of a random variable. Furthermore, uncertainty related to the load models is taken into account by introducing model uncertainty factors B_{global}, B_{load} and B_{sif}, where the latter is reflecting inaccuracies in the SIF calculation and used for the FM model only. These factors are random variables with distributions *LN(1,0.1)* for the first one and *LN(1,0.2)* for the other two. In addition, the influence of each important random variable in the calibration of partial factors is demonstrated in Table 4 where the ratio of the partial factors obtained from simulations over the partial factors of the reference case is considered, where the reference case is the value of Table 3 for a target reliability index equal to 3.8.

Table 3. Values of the partial factors

	$\beta_{target} \times \alpha_R$	$1.5 \times 0.8 = 1.2$	$3.1 \times 0.8 = 2.48$	$3.8 \times 0.8 = 3.04$	$4.3 \times 0.8 = 3.44$
Simulation	$failure\ probability_{target}$	11×10^{-2}	6.6×10^{-3}	1.2×10^{-3}	2.9×10^{-4}
	N_k	Partial Factors			
S-N, EN1993	5.31×10^6	0.88	1.17	1.32	1.43
S-N, BS7608	6.13×10^6	0.89	1.18	1.33	1.45
LEFM, Simplified law	4.76×10^6	0.79	1.06	1.19	1.31
LEFM, Bilinear law	4.71×10^6	0.78	1.09	1.25	1.36

Table 4. Description of the simulations for sensitivity analysis and their effects on partial factors

Simulation	Description		$\gamma_{simulation}/\gamma_{reference}$ for $\beta_{target} = 3.8$			
			$\alpha_R = 1$ for S5 and 0.8 for the rest			
	LEFM model	S-N model	SN, EN1993	SN, BS7608	FM, Simplified	FM, bilinear
S1	Deterministic initial crack size,	-	-	-	0.96	0.96
S2	Deterministic threshold value for ΔK	-	-	-	1.07	1.06
S3	Without considering the threshold value for ΔK	-	-	-	1.07	1.06
S4	Deterministic model parameters A_1 & A_2 or A	-	-	-	1.00	0.98
S5	Considering model uncertainty factors on loads	Considering model uncertainty factors on loads	1.16	1.17	2.21	2.11
S6	-	Deterministic material parameters a_1 & a_2 or c_0	0.97	0.98	-	-

The results of each simulation in the terms of failure probability and reliability index trends are presented in Fig. 3 and Fig. 4. In case of S-N models, considering a deterministic value for material parameters has a small effect on partial factors because in the region around the target reliability index, simulation S6 behaves similar to the reference case. But in the zone with higher failure probability, the differences become more considerable. On the other hand, introducing the model uncertainty factors to loads has a substantial effect in any case. In Fig. 4, it can be observed that curves related to simulations S2 and S3 coincide completely. The reason is that for this particular stress spectrum, the minimum value of ΔK for each CMCS sample is higher than the characteristic value of ΔK_{th}.
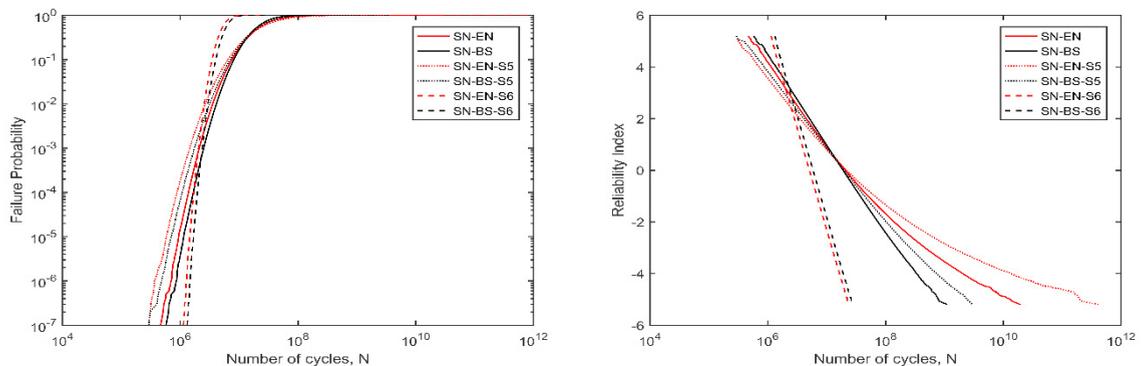
Fig. 3 Failure probability trend (Left) and Reliability index trend (Right) for sensitivity analysis of S-N models

Thus, using the characteristic value has the same influence on the reliability analysis as not considering the threshold value. As for S-N models, implementing the model uncertainty factors (S5) changes the behavior dramatically in all cases, while simulation S3 is in a good compatibility with the reference case, only in the zone that designers are generally interested in.
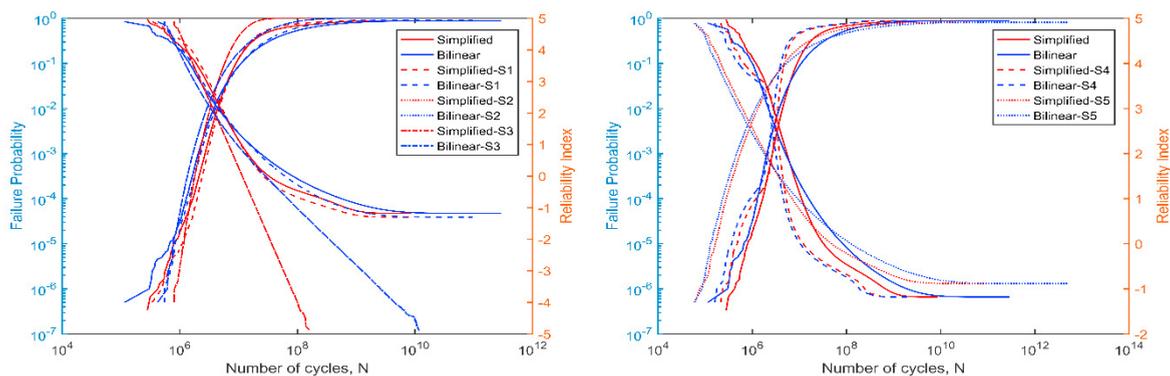
Fig. 4 Failure probability and reliability index trend for sensitivity analysis of LEFM models. S1, S2 & S3 (Left) S4 & S5 (Right)

5. Conclusion

In this paper the consistency in failure probability is compared between S-N curves proposed by BS and EN standards. For the considered stress range histogram, an acceptable agreement exists in the high cycle fatigue region but not in the very high cycle fatigue region that is often of interest to practical designs. Similarly, for the FM approaches a reasonable agreement is found in the high cycle fatigue region but not in the very high cycle fatigue region. This is due to threshold conditions being incompatible with the S-N curve format. The model uncertainties on loads have the highest impact on the outcome of the probabilistic assessment and reliability analyses. They should be determined with care.

References

EN 1993-1-9, European Committee for Standardization, *eurocode 3: design of steel structures, 2005*.

BS 7608, 2014. BSI Standards Publication: *Guide to fatigue design and assessment of steel products*.

Hobbacher, A.F., 1996. *Fatigue design of Welded joints and Components. Recommendation of IIW joint working group XIII-XV*. Woodhead Publishing. Paperback ISBN: 9781855733152

ISO 2394:2015, *General principles on reliability for structures*.

JCSS, 2001. Joint committee of structural safety, *Probabilistic Model Code*.

BS 7910, 2013. BSI Standards Publication: *Guide to methods for assessing the acceptability of flaws in metallic structures*.

DNV.GL-RP-0001, 2015. *Probabilistic methods for planning of inspection for fatigue cracks in offshore structures*.

Haibach, E., 1970. *The allowable stresses under variable amplitude loading of welded joints*. In proceeding of the conference on fatigue of welded structures, Vol. 2.

Niemi, E., 1997. *Random loading behavior of welded components*. In IIW international conference on performance of dynamically loaded welded structures, San Francisco.

Gurney, T.R., 2006. *Cumulative Damage of Welded Joints*, Woodhead Publishing. Hardcover ISBN: 9781855739383.

Kaplan, E. L., Meier, p., 1958. *Nonparametric estimation from incomplete observation*. American statistical association, 53(282), pp.457–481.

HSE, 1998. Health and Safety Executive report: *A review of fatigue crack growth rates in air and seawater, OTH511*.

Maljaars, J., Steenbergen, H.M.G.M. & Vrouwenvelder, A.C.W.M., 2012. *Probabilistic model for fatigue crack growth and fracture of welded joints in civil engineering structures*. International Journal of Fatigue, 38, pp.108–117.

EN 1990, European Committee for Standardization, *eurocode :Basis of structural design, 2002*,